

IODP Expedition 340T: Borehole Logging at Atlantis Massif Oceanic Core Complex

by Donna Blackman, Angela Slagle, Alistair Harding, Gilles Guerin, and Andrew McCaig

doi:10.2204/iodp.sd.15.04.2013

Abstract

Integrated Ocean Drilling Program (IODP) Expedition 340T returned to the 1.4-km-deep Hole U1309D at Atlantis Massif to carry out borehole logging including vertical seismic profiling (VSP). Seismic, resistivity, and temperature logs were obtained throughout the geologic section in the footwall of this oceanic core complex. Reliable downhole temperature measurements throughout and the first seismic coverage of the 800–1400 meters below seafloor (mbsf) portion of the section were obtained. Distinct changes in velocity, resistivity, and magnetic susceptibility characterize the boundaries of altered, olivine-rich troctolite intervals within the otherwise dominantly gabbroic sequence. Some narrow fault zones also are associated with downhole resistivity or velocity excursions. Small deviations in temperature were measured in borehole fluid adjacent to known faults at 750 mbsf and 1100 mbsf. This suggests that flow of seawater remains active along these zones of faulting and rock alteration. Vertical seismic profile station coverage at zero offset now extends the full length of the hole, including the uppermost 150 mbsf, where detachment processes are expected to have left their strongest imprint. Analysis of wallrock pro-

perties, together with alteration and structural characteristics of the cores from Site U1309, highlights the likely interplay between lithology, structure, lithospheric hydration, and core complex evolution.

Geologic Setting and Motivation

The Atlantis Massif oceanic core complex (OCC) was drilled during IODP Expedition 304/305 (Blackman et al., 2006). It formed due to spatial and temporal variability in magmatism and faulting within the axial zone of the slow-spreading Mid-Atlantic Ridge at 30°N (Cann et al., 1997). Long-lived strain localization along select axial faults allowed development of a detachment zone that unroofed intrusive crust 0.5–1.5 Ma (Grimes et al., 2008). High fracture intensity in the detachment zone enabled circulation of seawater (McCaig et al., 2010), and associated alteration included formation of low-strength minerals that enhanced strain localization. Geophysical studies (Blackman et al., 2008; Canales et al., 2008; Collins et al., 2009; Blackman and Collins, 2010; Henig et al., 2012), seafloor mapping and sampling (Blackman et al., 2002; Schroeder and John, 2004; Boschi et al., 2006; Karson et al., 2006), and deep basement drilling and logging (Blackman et al., 2011; Ildefonse et al.,

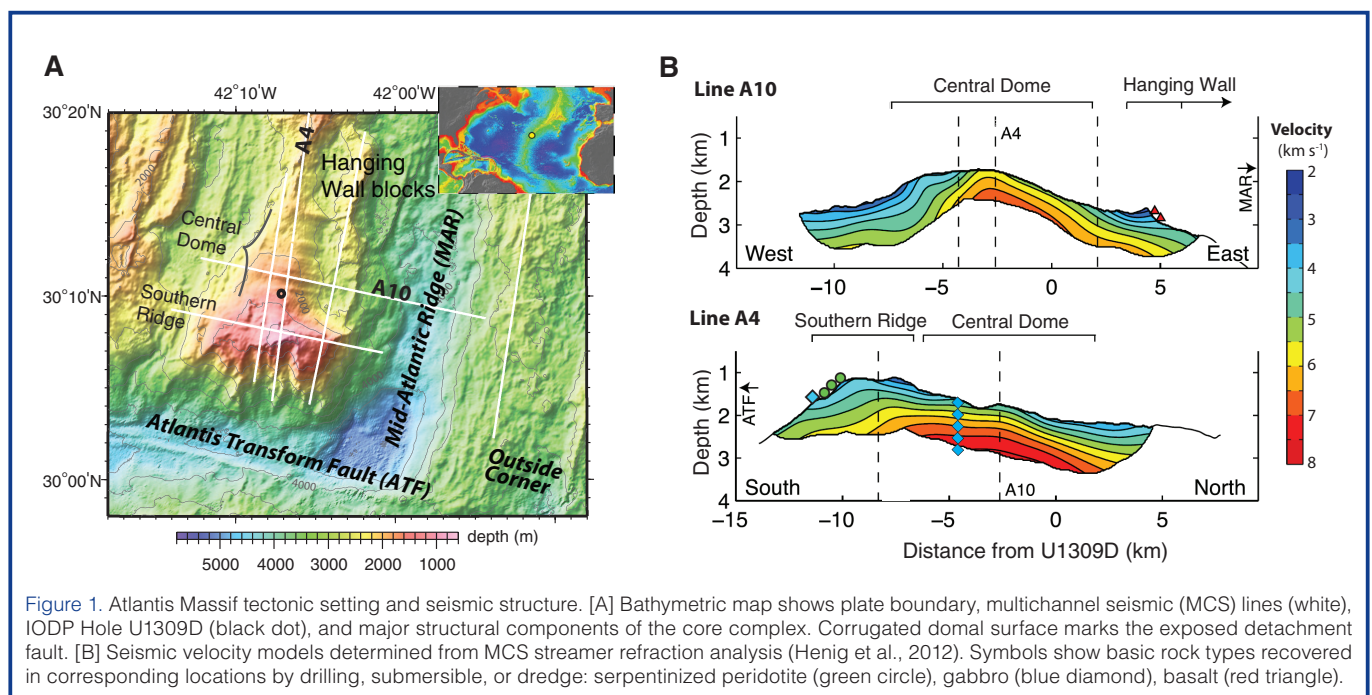


Figure 1. Atlantis Massif tectonic setting and seismic structure. [A] Bathymetric map shows plate boundary, multichannel seismic (MCS) lines (white), IODP Hole U1309D (black dot), and major structural components of the core complex. Corrugated domal surface marks the exposed detachment fault. [B] Seismic velocity models determined from MCS streamer refraction analysis (Henig et al., 2012). Symbols show basic rock types recovered in corresponding locations by drilling, submersible, or dredge: serpentinized peridotite (green circle), gabbro (blue diamond), basalt (red triangle).

2007) all contribute to the model of how the Atlantis Massif OCC evolved.

Figure 1 illustrates the structural components of the Atlantis Massif and the variability in shallow velocity field; a lack of a conventional seismic Layer 2 within the core complex is evident. The domal core is capped by the corrugated, exposed detachment fault that unroofed the intrusive crust drilled at Site U1309 on the Central Dome. This gabbroic body has seismic velocity of $5.5\text{--}7\text{ km s}^{-1}$ and shoals to the seafloor in the eastern part of the central and southern portions of the domal core (Henig et al., 2012). The exposed detachment fault bounds the high velocity gabbroic body on the east, dipping beneath the basaltic hanging wall blocks toward the axis of the Mid-Atlantic Ridge. The steeper, western boundary of the body may be an intrusive contact that was originally near horizontal, but other interpretations are also under investigation (Harding et al., 2012). Paleomagnetic results indicate that at least the upper 400 m, and likely the full 1.4-km section, of Hole U1309D has rotated a minimum of 45° counterclockwise about a horizontal axis that parallels the rift valley (Morris et al., 2009). Seven narrow fault zones (several centimeters to a few meters in scale) within the interval 100–1100 mbsf were documented within the core and by earlier logging data (Blackman et al., 2006; Hirose and Hayman, 2008; Michibayashi et al., 2008). But the limited extent of these faults might imply that they did not dominate the development of the OCC. An eighth fault was identified at 1346 mbsf from logs obtained during Exp. 340T. However, some of these narrow intervals are associated with notable downhole change in degree/style of alteration and wallrock properties, so the implications of this are a subject for further investigation in which the Exp. 340T logs will play a significant role (Blackman et al., 2012).

Prior multi-channel seismic imaging (Canales et al., 2004) and application of a novel wide-angle stacking method (Singh et al., 2004; Masoomzadeh et al., 2010) suggested that there is considerable seismic reflectivity within the footwall of this oceanic core complex. This was somewhat surprising given the dominantly gabbroic section recovered from Hole U1309D. The Exp. 340T logging program was designed to document whether olivine-rich, highly altered intervals, and/or narrow, possibly fluid-bearing fault zones within the formation might contribute to regional reflectivity, thus potentially enabling use of the seismic sections for assessing former and current hydrological flow fields within the OCC.

Logging Operations

On approach for the initial reentry of Hole U1309D during Exp. 340T (February 2012), we monitored the video carefully for possible fluid flow into/out of the well. No flow was apparent, and the reentry cone had just a light sediment cover accrued since the end of drilling operations in 2005. Hole U1309D was found to be in good condition, and an initial, minimal-disturbance borehole fluid temperature measurement was achieved on the first logging run into the borehole. The triple combination tool string employed for that run included the Modular Temperature Tool (MTT) that documented the borehole fluid temperature at centimeter-scale resolution. Additional temperature measurements were made during each subsequent logging run using a sensor in the logging cable head. All standard log measurements were recorded and are in excellent agreement with data from Exp. 304/305. Intervals that are out of bore or unusually ragged match those recognized during the 2004–2005 drilling. Electrical resistivity was measured with the High-Resolution Laterolog Array (HRLA) during Exp. 340T, a newer resistivity tool than that used during Exp. 304/305. The HRLA provides six resistivity measurements at different depths of penetration into the wall rock, including one measurement of the borehole fluid.

Seismic velocity was measured during Exp. 340T throughout the section. The 800–1400 mbsf interval that had not been possible to cover at the end of Exp. 305 was logged with the Dipole Shear Sonic Imager, which was run with a low frequency sequence that generated Stoneley waves in addition to compressional and shear waves. A zero-offset Vertical

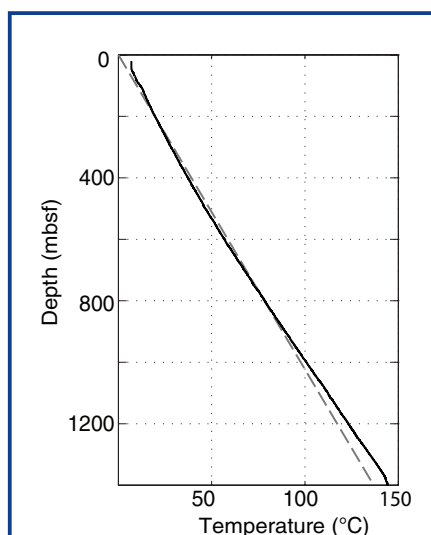


Figure 2. Borehole fluid temperature in Hole U1309D. Solid black line shows IODP 340T MTT measurements. Dashed gray line is predicted gradient at position of Site U1309 from 3-D model of plate-driven mantle flow and lithospheric cooling. The ridge-transform-ridge model had geometry and spreading rate of the study region (calculation of Blackman et al., 2008).

Seismic Profile (VSP) experiment was conducted using the *JOIDES Resolution* two-gun 250-in³ cluster as the source and the Versatile Seismic Imager (VSI) triaxial geophone as the receiver. The VSP was carried out during daylight hours over two days, in keeping with the marine mammal hazard mitigation plan. Differences in weather/ship conditions and problems with the VSI anchoring arm appear to have impacted data quality. High quality recordings were obtained during a VSP run when sea/wind state was calmest. The next day, most recordings had only fair signal-to-noise ratio, although initial analysis indicates that it will be possible to determine velocities to VSI stations throughout the section (Expedition 340T Scientists, 2012).

A newly constructed Magnetic Susceptibility Sonde (MSS) was run for the first time in seawater during Exp. 340T. Limits on operating temperature

restricted its use to the upper 750 mbsf. The data appear to be high quality, with intervals showing significant excursion in measured value agreeing closely with the multi-sensor track record of core susceptibility obtained during Exp. 304/305.

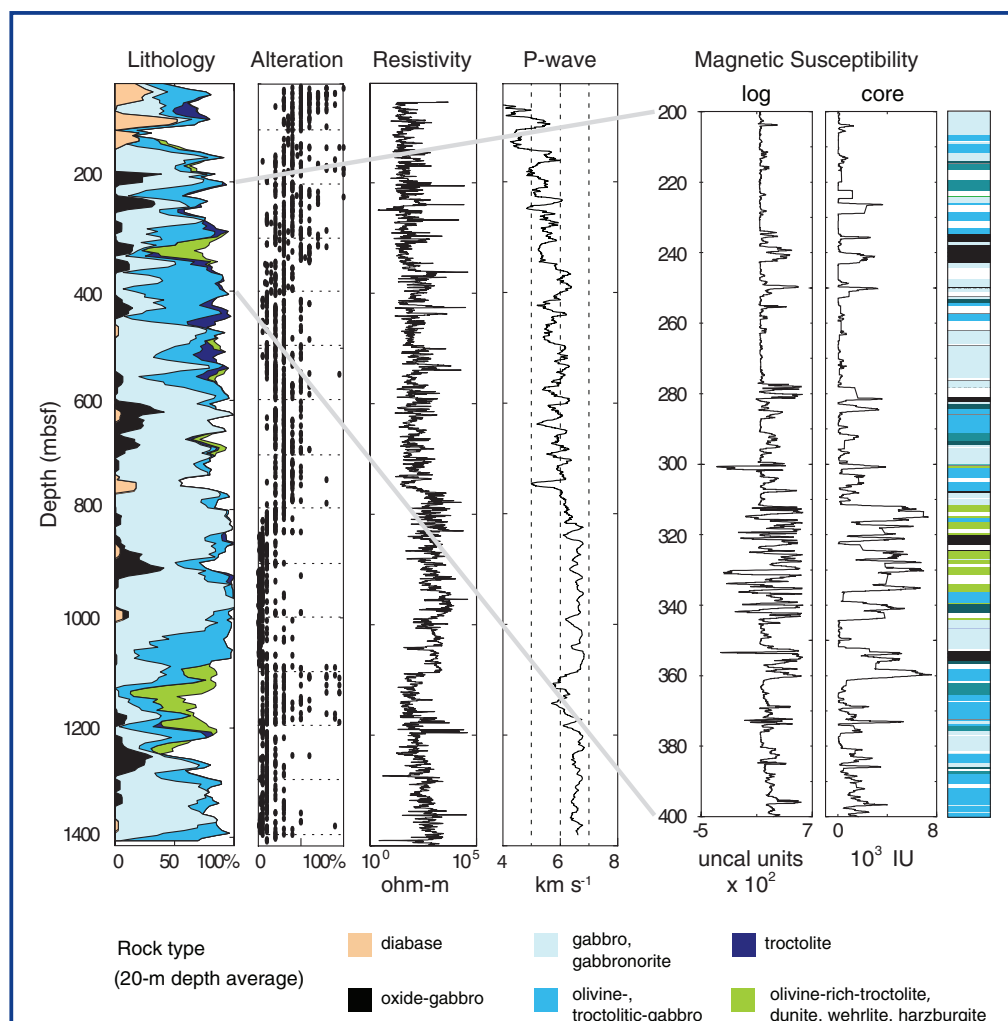
More detailed information on the logged properties, logging tools, and logging operations may be found in the IODP Exp. 340T Preliminary Report (Expedition 340T Scientists, 2012).

Highlighted Initial Results

Exp. 340T extended *in situ* seismic velocity measurement of intrusive oceanic crust, which typically comprises Layer 3, beyond one km, a depth where closure of micro-fractures eliminates bias associated with shallow exposure. Earlier work had documented gabbroic wallrock velocities to subsurface depths of 0.5–0.8 km (Itturino et al., 2002; Blackman et al., 2006). The new logs indicate that the little-altered section from 800 mbsf to 1400 mbsf at Site U1309 has a mean

compressional velocity of 6.6 km s⁻¹ and mean shear velocity of 3.7 km s⁻¹. These averages excludes the olivine-rich troctolite interval at 1080–1220 mbsf that has several highly serpen-tinized intervals. This multimeter-scale average represents the inherent seismic properties of this (and likely most oceanic) gabbroic section. When post-processing of the VSP data is complete, a site average compressional velocity for this intrusive crustal section will be obtained that includes the effects of fracturing at the 100-m scale that the sonic log does not measure.

The temperature at the base of Hole U1309D at 1400 mbsf is ~146°C. The downhole gradient (Fig. 2) is nearly linear—just under 100°C km⁻¹ (Expedition 340T Scientists, 2012)—but closer examination, after removing a linear trend, shows some interesting downhole thermal structure. Small deviations in borehole fluid temperature measured adjacent to a few narrow faults, documented in the core and/or Exp. 304/305 Formation MicroScanner (FMS) images, suggest that seawater presently percolates through these zones.



Integration of the new log data with a prior geologic description of Hole U1309D core indicates that boundaries of highly altered olivine-rich troctolite intervals mark distinct changes in seismic velocity, resistivity, and magnetic susceptibility within the gabbroic section (Fig. 3). There are two zones where olivine-rich troctolite occurs repeatedly throughout an interval that is tens of meters thick: 310–350 mbsf and 1080–1220 mbsf. Other ultramafic intervals are tens of centimeters to ~3 m thick, with dunite and harzburgite only recovered above 224 mbsf. A fault zone at 750 mbsf (Michibayashi et al., 2008) is also associated with a significant local drop in seismic velocity, and below it resistivity increases rapidly. This is one of the faults where a small deviation in borehole fluid temperature was confirmed during Exp. 340T, and another occurs at ~1100 mbsf. Both these faults were documented by deformation structures in core samples and by fault gouge. The ~1100 mbsf fault and another newly identi-

Figure 3. Downhole logs for IODP Hole U1309D. Lithology of core with white showing percent unrecovered core. Overall alteration based on Exp. 304/305 visual core description of individual core pieces. Borehole resistivity shows rapid change at ~350 mbsf, 750 mbsf, and 1080 mbsf. Borehole velocity, filtered with a 10-m running boxcar average. Detail of magnetic susceptibility from Exp. 340T logs (in uncalibrated units) and Exp. 304/305 core (25-pt running average), with detailed lithology, from 200 mbsf to 400 mbsf.

fied narrow fault zone at ~1345 mbsf have sharply distinct seismic properties that cause reflection of the borehole Stoneley wave (Fig. 4).

The thickness of the lower velocity interval associated with the altered olivine-rich troctolite zone at 1080–1220 mbsf is sufficient that, if laterally extensive, would be detectable within regional, far-field seismic data. Compressional velocities are 0.5–1 km s⁻¹ lower than the surrounding rock. Similarly, the olivine-rich troctolite interval at 310–350 mbsf has velocity notably lower than adjacent rock. Much of the section shallower than 350 mbsf is highly altered, so it is possible that structure or processes associated with the base of this olivine-rich troctolite zone are more relevant in controlling seismic properties than alteration within the zone itself. Nevertheless, there is a distinct drop of over 0.5 km s⁻¹ at 310 mbsf, the top of the zone, and an increase of ~1 km s⁻¹ below the base. The seismic velocity of the moderately altered section at 350–750 mbsf varies modestly around a value of ~6 km s⁻¹. As noted above, the little-altered section deeper than 800 mbsf has an average velocity of 6.6 km s⁻¹, with a maximum discrete velocity of ~6.8 km s⁻¹. Primary lithology would dictate that the highest velocities accompany the olivine-rich intervals, but we find that alteration plays the dominant role in determining present-day seismic velocity in the upper kilometer and a half of the domal core at Atlantis Massif.

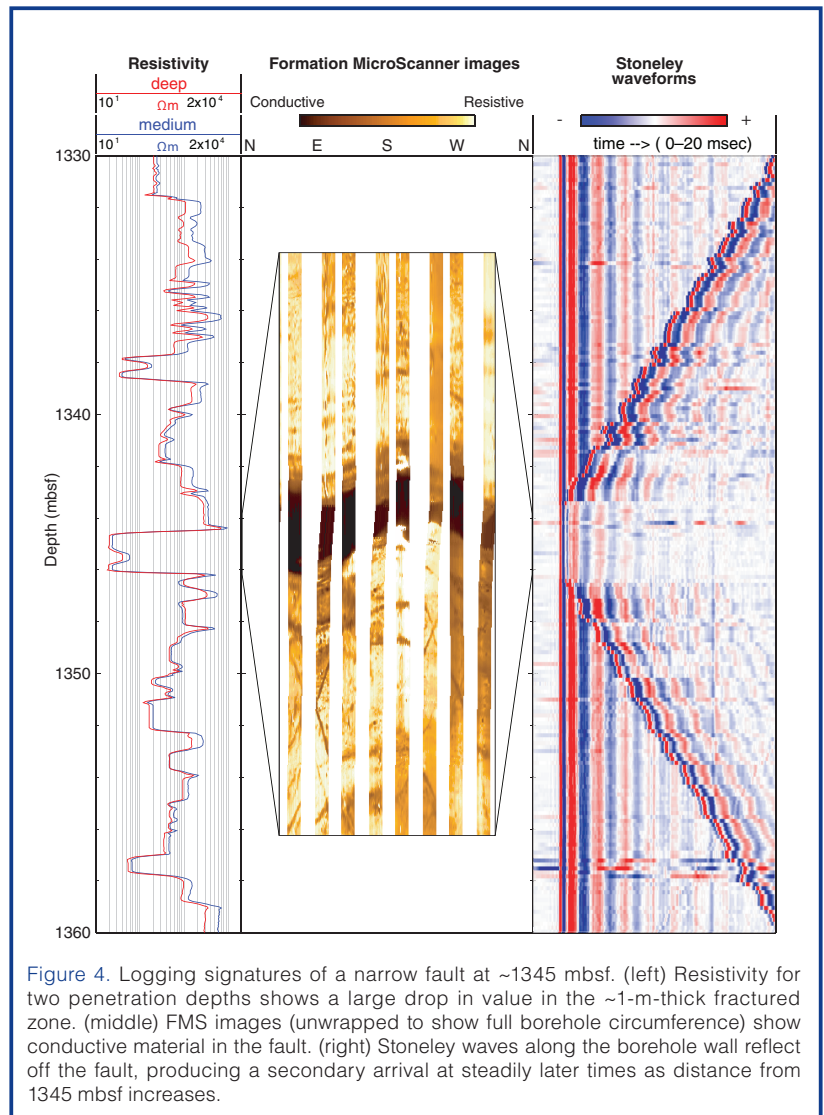


Figure 4. Logging signatures of a narrow fault at ~1345 mbsf. (left) Resistivity for two penetration depths shows a large drop in value in the ~1-m-thick fractured zone. (middle) FMS images (unwrapped to show full borehole circumference) show conductive material in the fault. (right) Stoneley waves along the borehole wall reflect off the fault, producing a secondary arrival at steadily later times as distance from 1345 mbsf increases.

References

- Blackman, D., Slagle, A., Guerin, G., and Harding, A., 2012. Formation and early evolution of oceanic lithosphere- multi-faceted study of tectonic, magmatic, and hydrologic processes at Atlantis Massif, MAR 30°N, [Paper presented at 2012 Fall Meeting AGU San Francisco, 3–7 December 2012]. Abstract OS44A-01
- Blackman, D. K., and Collins, J. A., 2010. Lower crustal variability and the crust/mantle transition at the Atlantis Massif oceanic core complex. *Geophys. Res. Lett.*, 37(24):L24303. doi:10.1029/2010GL045165
- Blackman, D. K., Ildefonse, B., John, B. E., Ohara, Y., Miller, D. J., Abe, N., Abratis, M., et al., 2011. Drilling constraints on lithospheric accretion and evolution at Atlantis Massif, Mid-Atlantic Ridge 30°N. *J. Geophys. Res.*, 116:B07103. doi:10.1029/2010JB007931
- Blackman, D. K., Ildefonse, B., John, B. E., Ohara, Y., Miller, D. J., MacLeod, C. J., and the Expedition 304/305 Scientists, 2006. *Proc. IODP, 304/305*: Washington, DC (Integrated Ocean Drilling Program Management International, Inc.). doi:10.2204/iodp.proc.304305.2006
- Blackman, D. K., Karner, G., and Searle, R. C., 2008. Three-dimensional structure of oceanic core complexes: Effects on gravity signature and ridge flank morphology, Mid-Atlantic Ridge 30°N. *Geochem. Geophys. Geosyst.*, 9:Q06007. doi:10.1029/2008GC001951
- Blackman, D. K., Karson, J. A., Kelley, D. S., Cann, J. R., Früh-Green, G. L., Gee, J. S., Hurst, S., et al., 2002. Geology of the Atlantis Massif (Mid-Atlantic Ridge, 30°N): Implications for the evolution of an ultramafic oceanic core complex. *Mar. Geophys. Res.*, 23(5–6):443–469. doi:10.1023/B:MARI.0000018232.14085.75
- Boschi, C., Früh-Green, G. L., Delacour, A., Karson, J. A., and Kelley, D. S., 2006. Mass transfer and fluid flow during detachment faulting and development of an oceanic core complex, Atlantis Massif (MAR 30°N). *Geochem. Geophys. Geosyst.*, 7(1):Q01004. doi:10.1029/2005GC001074
- Canales, J. P., Tucholke, B. E., and Collins, J. A., 2004. Seismic reflection imaging of an oceanic detachment fault: Atlantis megamullion (Mid-Atlantic Ridge, 30°10' N). *Earth Planet. Sci. Lett.*, 222(2):543–560. doi:10.1016/j.epsl.2004.02.023
- Canales, J. P., Tucholke, B. E., Xu, M., Collins, J. A., and Dubois, D. L., 2008. Seismic evidence for large-scale compositional heterogeneity of oceanic core complexes. *Geochem. Geophys. Geosyst.*, 9(8):Q08002. doi:10.1029/2008GC002009

- Cann, J. R., Blackman, D. K., Smith, D. K., McAllister, E., Janssen, B., Mello, S., Avgerinos, E., Pascoe, A. R., and Escartin, J., 1997. Corrugated slip surfaces formed at ridge–transform intersections on the Mid-Atlantic Ridge. *Nature*, 385:329–332. doi:10.1038/385329a0
- Collins, J. A., Blackman, D. K., Harris, A., and Carlson, R. L., 2009. Seismic and drilling constraints on velocity structure and reflectivity near IODP Hole U1309D on the central dome of Atlantis Massif, Mid-Atlantic Ridge 30°N. *Geochem. Geophys. Geosyst.*, 10(1):Q01010. doi:10.1029/2008GC002121
- Expedition 340T Scientists, 2012. Atlantis Massif Oceanic Core Complex. Velocity, porosity, and impedance contrasts within the domal core of Atlantis Massif: Faults and hydration of lithosphere during core complex evolution. *IODP Prel. Rept.*, 340T. doi:10.2204/iodp.pr.340T.2012
- Grimes, C. B., John, B. E., Cheadle, M. J., and Wooden, J. L., 2008. Protracted construction of gabbroic crust at a slow spreading ridge: Constraints from ²⁰⁶Pb/²³⁸U zircon ages from Atlantis Massif and IODP Hole U1309D (30°N, MAR). *Geochem. Geophys. Geosyst.*, 9(8):Q08012. doi:10.1029/2008GC002063
- Harding, A., Arnulf, A., and Expedition 340T Science Party, 2012. Crustal structure in the vicinity of Hole U1309D, Atlantis Massif [Paper presented at 2012 Fall Meeting AGU San Francisco, 3–7 December 2012]. Abstract OS11E-08.
- Henig, A. S., Blackman, D. K., Harding, A. J., Canales, J. P., and Kent, G. M., 2012. Downward continued multi-channel seismic refraction analysis of Atlantis Massif oceanic core complex, 30°N Mid-Atlantic Ridge. *Geochem. Geophys. Geosyst.*, 13(5):Q0AG07. doi:10.1029/2012GC004059
- Hirose, T., and Hayman, N. W., 2008. Structure, permeability, and strength of a fault zone in the footwall of an oceanic core complex, the Central Dome of the Atlantis Massif, Mid-Atlantic Ridge, 30°N. *J. Struct. Geol.*, 30(8):1060–1071. doi:10.1016/j.jsg.2008.04.009
- Ildefonse, B., Blackman, D. K., John, B. E., Ohara, Y., Miller, D. J., MacLeod, C. J., and IODP Expeditions 304/305 Science Party, 2007. Oceanic core complexes and crustal accretion at slow-spreading ridges. *Geology*, 35:623–626.
- Itturino, G. J., Ildefonse, B., and Boitnott, G., 2002. Velocity structure of the lower oceanic crust: Results from Hole 735B, Atlantis II Fracture Zone. In Natland, J. H., Dick, H. J. B., Miller, D. J., and Von Herzen, R. P., *Proc. ODP, Sci. Results*, 176: College Station, TX (Ocean Drilling Program), 1–71.
- Karson, J. A., Früh-Green, G. L., Kelley, D. S., Williams, E. A., Yoerger, D. R., and Jakuba, M., 2006. Detachment shear zone of the Atlantis Massif core complex, Mid-Atlantic Ridge, 30°N. *Geochem. Geophys. Geosyst.*, 7(6):Q06016. doi:10.1029/2005GC001109
- Masoomzadeh, H., Barton P. J., and Singh, S. C., 2010. Non-stretch moveout correction of long-offset multi-channel seismic data for subbasalt imaging: Example from the North Atlantic. *Geophysics*, 75(4):R83–R91. doi:10.1190/1.3443579
- McCaig, A. M., Delacour, A., Fallick, A. E., Castelain, T., and Früh-Green, G. L., 2010. Fluid circulation and isotopic alteration in and beneath oceanic detachment faults in the Central Atlantic: Implications for the geometry and evolution of high-temperature hydrothermal circulation cells at slow-spreading ridges. In Rona, P. A., Devey, C. W., Dymont, J., and Murton, B. J. (Eds.), *Diversity of Hydrothermal Systems on Slow Spreading Ocean Ridges*. AGU Geophys. Monogr. Ser., 188:207–239.
- Michibayashi, K., Hariagane, Y., Escartin, J., Delius, H., Linek, M., Hirose, T., Nozaka, T., and Ohara, Y., 2008. Hydration due to high-T brittle failure within in situ oceanic crust, 30°N Mid-Atlantic Ridge. *Earth Planet. Sci. Lett.*, 275(3–4):348–354. doi:10.1016/j.epsl.2008.08.033
- Morris, A., Gee, J. S., Pressling, N., John, B. E., MacLeod, C. J., Grimes, C. B., and Searle, R. C., 2009. Footwall rotation in an oceanic core complex quantified using reoriented Integrated Ocean Drilling Program core samples. *Earth Planet. Sci. Lett.*, 287(1–2):217–228. doi:10.1016/j.epsl.2009.08.007
- Schroeder, T., and John, B. E., 2004. Strain localization on an oceanic detachment fault system, Atlantis Massif, 30°N, Mid-Atlantic Ridge. *Geochem. Geophys. Geosyst.*, 5(1):Q11007. doi:10.1029/2004GC000728
- Singh, S. C., Collins, J. A., Canales, J. P., Tucholke, B. E., and Detrick, R. S., 2004. New insights into serpentinization at Atlantis Massif using wide-angle seismic method. *Eos Trans. AGU*, 85(47, Fall Meet. Suppl.):V23B-0628.

Authors

Donna Blackman, and **Alistair Harding**, Scripps Institution of Oceanography, University of California San Diego, 9500 Gilman Drive, La Jolla, CA 92093, U.S.A., e-mail: dblackman@ucsd.edu

Angela Slagle, and **Gilles Guerin**, Lamont Doherty Earth Observatory, Columbia University, 61 Route 9W, P.O. Box 1000, Palisades, NY 10964-8000, U.S.A.

Andrew McCaig, School of Earth and Environment, Maths/Earth and Environment Building, The University of Leeds, Leeds LS2 9JT, U.K.